

Sediment transport in ~~Indian~~ South Asian rivers high enough to impact satellite gravimetry

Alexandra Klemme¹, Thorsten Warneke¹, Heinrich Bovensmann¹, Matthias Weigelt², Jürgen Müller², Tim Rixen³, Justus Notholt¹, and Claus Lämmerzahl⁴

¹Institute of Environmental Physics, University of Bremen, Otto-Hahn-Allee 1, 28359 Bremen, Germany

²Institute of Geodesy, Leibniz Universität Hannover, Schneiderberg 50, 30167 Hannover, Germany

³Leibniz Center for Tropical Marine Research, Fahrenheitstr. 6, 28359 Bremen, Germany

⁴Centre of Applied Space Technology and Microgravity, University of Bremen, Am Fallturm 2, 28359 Bremen, Germany

Correspondence: A. Klemme (aklemme@uni-bremen.de)

Abstract. Satellite gravimetry is used to study the global hydrological cycle. It is a key component in the investigation of groundwater depletion on the Indian subcontinent. Terrestrial mass loss caused by river sediment transport is assumed to be below the detection limit in current gravimetric satellites of the Gravity Recovery and Climate Experiment Follow-On mission. Thus, it is not considered in the calculation of terrestrial water storage (TWS) from such satellite data. However, the Ganges and Brahmaputra rivers, which drain the Indian subcontinent, constitute one of the world's most sediment rich river systems. In this study, we estimate the impact of sediment mass loss within their catchments on ~~gravimetric estimates of trends in the local mass equivalent water height (EWH)~~ local trends in gravity and consequential estimates of TWS trends. We find that for the Ganges-Brahmaputra-Meghna catchment, sediment transport accounts for $(4 \pm 2)\%$ of the gravity decrease ~~that is~~ currently attributed to groundwater depletion. The sediment is mainly eroded from the Himalayas, where correction for ~~the~~ sediment mass loss reduces the decrease in ~~EWH by 0.22 cm yr^{-1} , which is about 14% of the EWH trend observed in that region~~ TWS by $0.22 \text{ cm of equivalent water height per year (14\%)$. However, ~~with~~ sediment mass loss in the Brahmaputra catchment ~~resulting to be~~ is more than twice that in the Ganges catchment ~~and sediment mainly being~~, and sediment is mainly eroded from mountain regions. Thus, the impact on gravimetric ~~EWH data~~ TWS trends within the Indo-Gangetic plain ~~is~~ the main region identified for groundwater depletion ~~is~~ results to be comparatively small ($< 2\%$).

15 1 Introduction

Since March 2002, the Gravity recovery and Climate Experiment (GRACE) provides satellite based measurements of the Earth's gravity field (Dahle et al., 2019), with the only major data gap being between the end of the original satellite mission in August 2017 and the launch of the follow-on mission (GRACE-FO) in May 2018. Gravity fields derived from satellite measurements yield information on global mass variations, which have proven crucial to monitor changes in global water storage and fluxes (Rodell et al., 2018). Retrieved data of the mass equivalent water height (EWH) are widely used for studies on ~~e.g. topics such as~~ glacier melting (Jacob et al., 2012; Luthcke et al., 2013), groundwater depletion (Rodell et al., 2009; Xie et al., 2020) and sea level rise (Cazenave et al., 2009; Jeon et al., 2018).

One significant region that yields ~~a negative EWH trend~~ negative trends in terrestrial water storage (TWS) is north-west India with an average decrease of $(29 \pm 2.5) \text{ m}^3 \text{ H}_2\text{O yr}^{-1}$ (Rodell et al., 2018; Xie et al., 2020). Several studies have investigated this decrease and ~~explain~~ explained it by a large-scale groundwater loss due to excessive extraction for irrigation (Tiwari et al., 2009; Rodell et al., 2009; Panda and Wahr, 2016; Rodell et al., 2018; Xie et al., 2020). Wada et al. (2012) found that the use of non-renewable groundwater for irrigation more than tripled since 1960. In the year 2000, one-fifth of the global irrigation water demand was fed by non-renewable groundwater abstraction, with the majority being abstracted in India and Pakistan (Wada et al., 2012). Furthermore, the depletion in Indian groundwater occurred during a period of increased precipitation, implying an even stronger water deficit for future droughts (Rodell et al., 2018).

A large fraction of the Indian subcontinent is drained by the Ganges-Brahmaputra river system. The Ganges and Brahmaputra rivers originate in the Himalayan belt and drain intensely cultivated regions before their confluence in Bangladesh and discharge into the Bay of Bengal (Subramanian and Ramanathan, 1996; Garzanti et al., 2011). These rivers are one of the largest source of water and sediment to the world's ocean (Akter et al., 2021). The high amounts of sediment they carry into the Bay of Bengal make up the Bengal Delta and Submarine Fan that extends from Bangladesh to south of the equator and contains at least $1.1 \cdot 10^{19} \text{ kg}$ of sediment with an average accumulation rate of $665 \cdot 10^9 \text{ kg yr}^{-1}$ (Curry, 1994). The sediment transport by the Ganges-Brahmaputra river system shows strong diurnal, seasonal ~~and annual variations (Subramanian and Ramanathan, 1996)~~ and estimates, and inter-annual variations (Subramanian and Ramanathan, 1996). Estimates of sediment discharge vary widely between $200 \cdot 10^9 \text{ kg yr}^{-1}$ and $1,600 \cdot 10^9 \text{ kg yr}^{-1}$ for the Ganges River (Rahman et al., 2018; Holeman, 1968) and between $150 \cdot 10^9 \text{ kg yr}^{-1}$ and $1,157 \cdot 10^9 \text{ kg yr}^{-1}$ for the Brahmaputra River (Akter et al., 2021; Milliman and Meade, 1983). Yet, recent studies state the annual combined sediment discharge of the rivers to be about 10^{12} kg with the majority being carried during the monsoon season from June to October (Wasson, 2003; Kuehl et al., 2005; Wilson and Goodbred, 2015; Mouyen et al., 2018; Mahmud et al., 2020; Akter et al., 2021).

This river sediment transport implies a terrestrial mass reduction that has so far not been considered in the computation of gravimetric ~~EWH-TWS~~ data. A study by Schnitzer et al. (2013) found that the mass loss associated with the large-scale soil erosion in the Chinese Loess Plateau was not visible considering the available GRACE resolution. However, recent studies found the sediment discharge to the ocean to be visible using satellite gravimetry of the estuary regions (Mouyen et al., 2018; Li et al., 2022). While the incorporation of sediment mass loss into monthly GRACE solutions over land might be impossible at the current satellite resolutions, it is a non-negligible loss when considering long term ~~EWH-TWS~~ trends studied in regard to e.g. groundwater depletion.

Additional processes to consider in long-term gravimetric data are plate tectonics. The Himalaya mountain range experiences uplift due to the tectonic collision between the Indian and the Eurasian continental plates. The gravimetric impact of this process is not the focus of this study. Yet, knowledge of such additional tectonic process is essential to contextualize the resulting sediment impact, as the increase in mass due to this Himalayan mountain uplift could counteract part of the mass loss due to sediment erosion and discharge.

In this study, we estimate ~~the this~~ impact of mass loss due to soil erosion and sediment transport by major rivers draining the Indian subcontinent on ~~EWH-TWS~~ trends observed by the GRACE and GRACE-FO satellites. ↵

2 Methods

2.1 Study Area

60 This study focuses on the Ganges and Brahmaputra catchments, with some discussion of the Indus and Meghna catchments. The rivers are located mainly in Northern India but also partly flow through China, Pakistan, Nepal, Bhutan, Afghanistan and Bangladesh (Figure 1). The river catchments are impacted by the South Asian monsoon, bringing high precipitation and river discharge from June to October, ~~whereat the south-eastern parts of the catchments are effected earlier and longer than the north-western parts.~~ The Ganges and Brahmaputra rivers originate in the Himalayan mountain belt and discharge into the Bay of Bengal after confluence with the Meghna river in Bangladesh. Together with the Indus River, they drain the majority of the Himalayas ~~(-)~~.

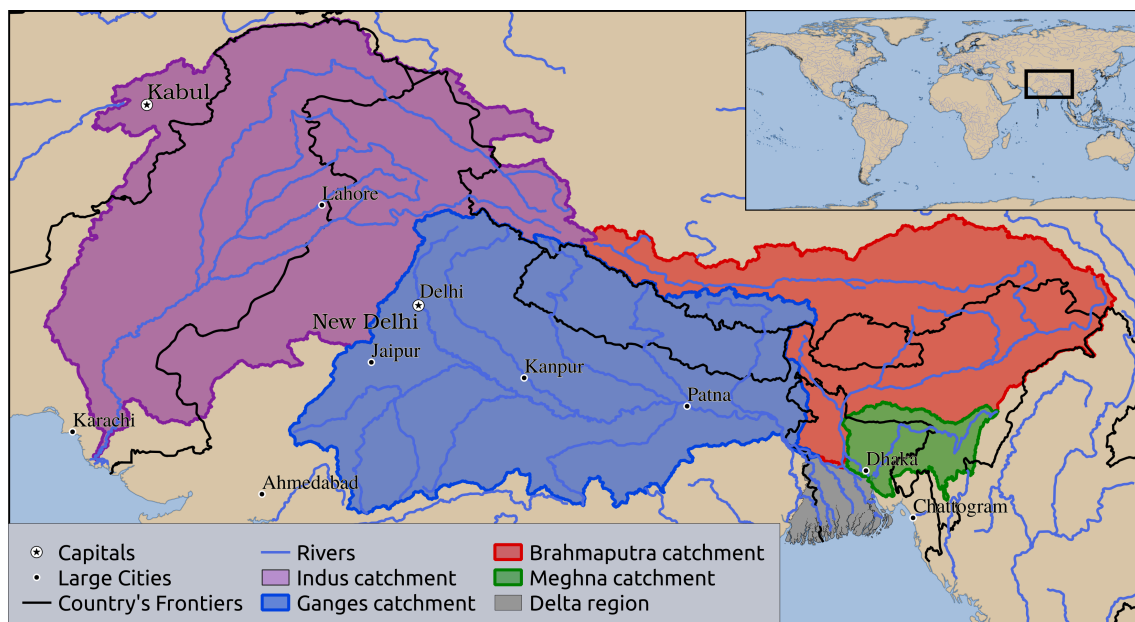


Figure 1. [Map of investigated catchments \(Lehner and Grill, 2013\) and river paths \(GRDC, 2020\).](#)

Due to high erosion rates in the Himalayan mountain region, sediment concentrations in ~~the these~~ rivers are among the highest worldwide (Subramanian and Ramanathan, 1996; Akter et al., 2021). ~~More Especially the Brahmaputra catchment has a large mountain fraction, while the other river catchments show higher agricultural fractions~~ (Table 1). ~~A map including the locations of mountain ranges and agricultural land as well as more~~ detailed river descriptions are included in the supplemental material.

~~Map of investigated catchments and river paths as well as indicated areas of mountain (elevation ≥ 1500 m) and agricultural regions. Elevation data is from Jarvis et al. (2008), agriculture regions are from GLCNMO (2017), river paths are from GRDC (2020) and river catchments are from Lehner and Grill (2013).~~

75 India hosts the world's largest groundwater-reliant agricultural irrigation system (Xie et al., 2020). Of its total irrigation-equipped area ($620,000 \text{ km}^2$), about 64% can be irrigated with groundwater, amounting to a total consumptive groundwater use for irrigation of about $200 \text{ km}^3 \text{ yr}^{-1}$ (Siebert et al., 2010). The fraction of irrigation reliant on groundwater has increased over the past decades from only 29% in 1951 to more than 50% in 2022 (FAO, 2022), with the absolute groundwater irrigated area being more than 5 times larger than in 1951 (Siebert et al., 2010; FAO, 2022). The major groundwater aquifer for the
80 studied regions is located in the Indo-Gangetic Plain and stretches mainly beneath the Indus and Ganges floodplains, while there are only shallow aquifers in the Himalayan mountain regions ([Supplemental supplemental Figure S2](#)).

~~This study specifically focuses on catchment fractions that are 1) utilized for agriculture or 2) located in erosion-prone mountain regions of elevations $\geq 1,500$ m. The Ganges catchment includes 65.2% agricultural area and 15.9% mountain area (-). The Brahmaputra catchment includes 18.2% agricultural area and 67.4% mountain area. In total, 36% of the studied region
85 are located in the mountains and 39.3% are used for agriculture (-).~~

Table 1. Mountain and agricultural fractions of the catchments.

	Total	GBM	Ganges	Brahmaputra	Meghna	Indus
catchment area (km^2)	2,679,070-069	1,576,135-134	950,754	539,989	5885,391	864,452-1,102,935
mountain fraction (%)	36.0	32.9	15.9	67.4	3.3	51.6
agricultural fraction (%)	45.6	39.3	65.2	18.2	42.8	34.4

Total refers to the combined Ganges, Brahmaputra, Meghna and Indus catchments. GBM is the Ganges-Brahmaputra-Meghna catchment. Mountain fraction refers to regions of elevation $\geq 1,500$ m (based on elevation data from Jarvis et al., 2008). Agricultural regions are from GLCNMO (2017). River catchment data are from Lehner and Grill (2013).

2.2 Gravimetry and sediment data

Gravimetry data in this study is from the GRACE and GRACE-FO satellites. We use post-processed data from the Combination International Service for Time-variable Gravity Fields (COST-G) Level 3 data product (Boergens et al., 2020) for ~~terrestrial~~
~~water storage-TWS~~ anomalies in units of EWH. The data are based on the COST-G RL01 Level 2B products by Dahle and
90 Murböck (2020) and include gridded data for ~~EWH, EWH-TWS, TWS~~ uncertainty, spatial leakage contained in the ~~EWH~~
~~TWS~~ and the background model atmospheric mass, all in a monthly resolution of $1^\circ \times 1^\circ$. The potential impact of filtering and spatial leakage in these data is discussed in the Supplemental Material.

Monthly ~~EWH-TWS~~ anomalies within the investigated catchments are derived by selecting all data whose grid centers are located within the respective catchment and calculating their area weighed average for each month. Data uncertainty is derived
95 analogously from the area-weighted average of the ~~EWH-TWS~~ uncertainties provided in the COST-G data product. Linear least-squares optimizations of the generated monthly time-series yield the local ~~EWH-TWS~~ trends. Trend uncertainties contain

the standard error of the derived slope optimization as well as the uncertainty of the monthly time series. [A more detailed trend analysis is included in the supplemental material.](#)

100 Sediment data for this study were collected from the literature. Generally, measurements in the study area are scarce and existing data is located close to Bangladesh, providing no information on the areal distribution of sediment loss in the upper catchments. The Supplemental Material provides a discussion on this scarcity in sediment data and the consequences for our study. Complete lists of the sediment data and their sources for the Ganges and Brahmaputra rivers are available in the supplemental tables S1 and S2, respectively.

3 Results & Discussions

105 3.1 Geodetic observations of the decrease in ~~equivalent terrestrial water height~~storage

Gravimetric data of ~~EWHTWS~~EWHTWS generally show negative trends within the studied catchments. Trends are most pronounced in the eastern Brahmaputra catchment and in the western Ganges catchment at the border to the Indus catchment. The data yields the strongest decline of 5.8 cm yr^{-1} in north-west India at about 28°N and 76°E (Figure 2).

110 ~~Trend of equivalent water height (EWH) with location of major river basins on the Indian subcontinent. Data were derived from linear least-squares approximation of the COST-G data (Boergens et al., 2020), based on the GRACE and GRACE-FO time period of 04-2002 to 12-2021. Location of river catchments are from Lehner and Grill (2013).~~

Comparison of average ~~EWHTWS~~EWHTWS trends within the individual catchments ~~yields yield~~ the strongest decrease for the Ganges catchment, followed by the Brahmaputra and Indus catchments. The Meghna catchment shows the weakest ~~EWHTWS decrease trend~~ (Table 2). Low standard deviation of trends in the Brahmaputra and Meghna catchments imply rather homogeneous 115 distributions of the ~~EWHTWS~~EWHTWS decrease in those catchments (Table 2). ~~In Higher standard deviations in the Ganges and Indus catchments, standard deviations are higher (1.7 cm yr^{-1} and 1.5 cm yr^{-1} compared to 0.6 cm yr^{-1} and 0.4 cm yr^{-1}) because the strong trends in those regions are~~ (Table 2) ~~are likely~~ caused by the distinct negative trend in north-west India. This is confirmed further by the comparatively low median trend values within these catchments (Table 2).

120 ~~Additional assessment of TWS trends in catchment mountain regions yields similar results for the Ganges and the Brahmaputra catchments (Table 2). For the Brahmaputra catchment, the observed TWS decrease is slightly higher than for the catchment average. For the Ganges catchment, it is slightly lower than the catchment average (Table 2). While the center of the main TWS decrease in the Ganges catchment is located in the Indo-Gangetic plain, it extends into the Ganges mountain ranges. This implies that the TWS decrease in the Ganges mountain regions could be overestimated due to the impact of TWS leakage caused by data filtering, as discussed in the Supplemental Material.~~

125 ~~Additional assessment of EWH trends in catchment mountain regions yields similar results for the Ganges and the Brahmaputra catchments (1.6 cm yr^{-1} , -). For the Brahmaputra catchment, the observed EWH decrease is slightly higher than for the catchment average. For the Ganges catchment, it is slightly lower than the catchment average (-). While the center of the main EWH decrease in the Ganges catchment is located in the Indo-Gangetic plain, it extends into the Ganges mountain ranges.~~

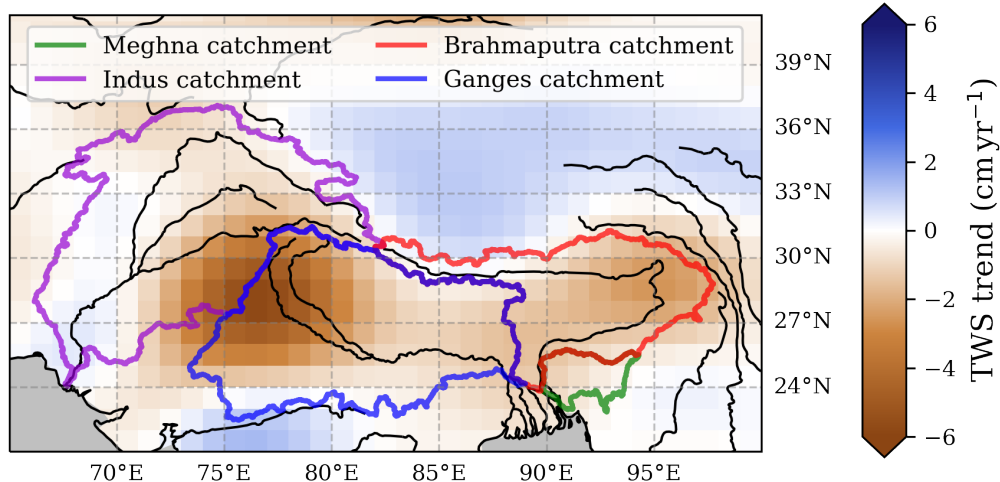


Figure 2. Trend of satellite based terrestrial water storage (TWS) with location of major river basins on the Indian subcontinent. Data were derived from linear least-squares approximation of the COST-G data (Boergens et al., 2020), based on the GRACE and GRACE-FO time period of 04-2002 to 12-2022. Location of river catchments are from Lehner and Grill (2013).

Table 2. Loss of equivalent terrestrial water height storage within the catchments.

<u>EWHTWS</u> loss (cm yr ⁻¹)	Total	GBM	Ganges	Brahmaputra	Meghna	Indus	Ganges-m	Brahmaputra-m
mean	1.35	1.51	1.63	1.45	0.60	1.13	1.56	1.60
median	1.09	1.32	1.24	1.46	0.62	0.57	1.30	1.68
standard deviation	1.43	1.36	1.67	0.64	0.35	1.49	0.71	0.66
minimum	-1.12	-1.12	-1.12	0.27	0.09	-0.48	0.94	0.28
maximum	5.78	5.77	5.77	2.64	1.17	5.78	3.40	2.64

Data show the loss of TWS in cm of equivalent water height per year. Negative values represent a water increase. GBM is the combined Ganges-Brahmaputra-Meghna catchment. Total refers to the combination of the Ganges, Brahmaputra, Meghna, and Indus catchments. Ganges-m and Brahmaputra-m refer to the mountain regions (altitude $\geq 1,500$ m) within the Ganges and Brahmaputra catchment, respectively. Data was derived based on pixel-wise linear least-squares fit of the COST-G GACE data. The mean values are weighed by the different pixel areas while the other statistical variables do not consider respective pixel sizes.

130 ~~This implies that the EWH decrease in the Ganges mountain regions could be overestimated due to the impact of EWH leakage caused by data filtering, as discussed in the Supplemental Material.~~

For the combined study area, the average ~~EWHTWS decrease derived from satellite data~~ is (1.4 ± 0.2) cm yr⁻¹. The time series of EWHTWS in the study area decreases fairly linear with annual variations, mainly driven by precipitation patterns that cause increasing EWHTWS during the monsoon months and decreasing EWHTWS during dry periods (Figure 3, ~~Supplemental Material~~). This EWHTWS decrease over the complete study area of $2.68 \cdot 10^6$ km² ~~represents a water represents~~
 135 ~~a~~ mass reduction of $36 \cdot 10^{12}$ kg yr⁻¹ ~~observed by gravimetry~~.

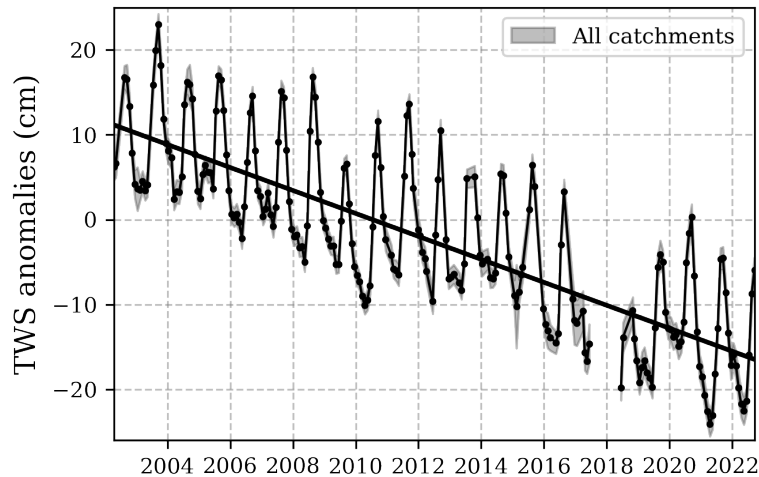


Figure 3. Time series of equivalent-average terrestrial water height-storage (EWH-TWS) anomalies within the total-combined Ganges, Brahmaputra, Meghna, and Indus catchments. Data points are area weighed monthly averages within the catchments and shaded areas represents area weighed uncertainties stated in the COST-G data product (Boergens et al., 2020). The linear trend was derived based on ordinary least-squares optimization of monthly data. The data gap represents the time between the end of the initial GRACE mission and the start of the GRACE-FO mission.

3.2 Mass loss caused by river sediment transport

To estimate the impact of sediment transport on the observed trend in gravity anomalies, we need the total sediment discharge from the studied regions. Based on data collected in various studies, the annual sediment discharge from the Ganges and Brahmaputra rivers is $501 \cdot 10^9 \text{ kg yr}^{-1}$ and $596 \cdot 10^9 \text{ kg yr}^{-1}$, respectively (Table 3). Sediment discharge from the Indus River is $168 \cdot 10^9 \text{ kg yr}^{-1}$ and the Meghna River discharges $11 \cdot 10^9 \text{ kg}$ of sediment per year (Table 3). The high sediment values in the Ganges and Brahmaputra rivers are caused by their origin in the Himalayan mountains, as those are highly erosion prone regions. The Meghna river originates in the Indian Naga Hills at less than 2,000m elevation and mainly drains the floodplains. The Indus river originates in the Himalayas. However, its annual sediment discharge has been strongly reduced by the installment of dams along the river.

145 ~~Considering seasonality in sediment discharge based on water discharge stated in Islam (2016), more than 80% of the sediment is transported~~ Due to data scarcity, it is difficult to assess spatially resolved data for sediment induced gravity changes in the Indian subcontinent. In the following, we separate between sediment eroded from specific mountain regions based on published literature (Wasson, 2003; Galy et al., 2007; Faisal and Hayakawa, 2022). Additionally, a discussion of spatially resolved sediment loss based on soil loss data from the Revised Universal Soil Loss Equation (RUSLE, Borrelli et al., 2017) is
 150 included in the Supplemental Material.

Table 3. River sediment transport within the catchments.

sediment load (10^9 kg yr^{-1})	Total	GBM	Ganges	Brahmaputra	Indus	Meghna
mean	1,276	2,008	501	596	168	11
median	1,207	1,082	480	590	125	12
standard deviation	633	511	272	237	122	2
minimum	400	350	200	150	50	0
maximum	3,147	2,777	1,600	1,157	370	20

Sediment loads as compiled from the literature. Total refers to the sum of sediment discharge in all four rivers. GBM refers to sediment discharge in the Ganges-Brahmaputra-Meghna river system. The complete lists of data compiled for the Ganges and Brahmaputra rivers are in the Supplemental Material in Table S2 and Table S3, respectively. Sediment load in the Meghna River is compiled from Coleman (1969), Smith et al. (2009), and Rahman et al. (2018). Sediment load in the Indus River is compiled from Holeman (1968), Milliman and Meade (1983), Giosan et al. (2006), and Mouyen et al. (2018).

The majority of sediment is discharged during the monsoon season from June to October, when there is also high water discharge in the rivers (Islam, 2016). Over the considered period of GRACE measurements (2002–2022), the rivers discharged more than 25 Pg of sediment. The average discharge rate is roughly $1.3 \cdot 10^{12} \text{ kg yr}^{-1}$ (Supplemental Material). These periods of high sediment discharge correlate with the time of increasing EWH. Thus Table 3).

155 3.3 Discussion of data seasonality

The seasonality of both TWS anomalies and river sediment discharge depends on the South Asian monsoon. As such, both parameters follow the seasonality of regional precipitation with the sediment discharge peaking approximately one month after the precipitation maximum and the TWS peaking one month after that (Figure 4). Since the monsoon moves from south-east over the Indian subcontinent, precipitation in the Brahmaputra and Meghna catchments start to increase earlier in the year and more gradually, while precipitation in the Ganges and Indus catchments start later and increases more rapidly.

This difference in precipitation patterns is also visible in the sediment discharge and TWS anomalies. For the Brahmaputra River, sediment discharge and TWS in the river catchment yield minima in February and show a gradual increase until the monsoon peak in July (Figure 4). After that, sediment discharge decreases with the precipitation decrease, while TWS stays high until October, when precipitation rates drop below 5 mm day^{-1} . Parameters in the Meghna catchment follow a similar seasonality, whereat precipitation and TWS anomalies are more pronounced in that catchment. Yet, sediment discharge is by an order of magnitude weaker than in the Brahmaputra catchment.

For the Ganges River, sediment discharge increases from June to August and decreases from September to November. TWS anomalies in the Ganges catchment increase between June and August and show a steady decline from September to June, when the precipitation rate is below 6 mm day^{-1} (Figure 4). In the Indus catchment, precipitation rates and TWS anomalies show only small changes during the monsoon season. Additionally, these parameters yield a second local maximum between

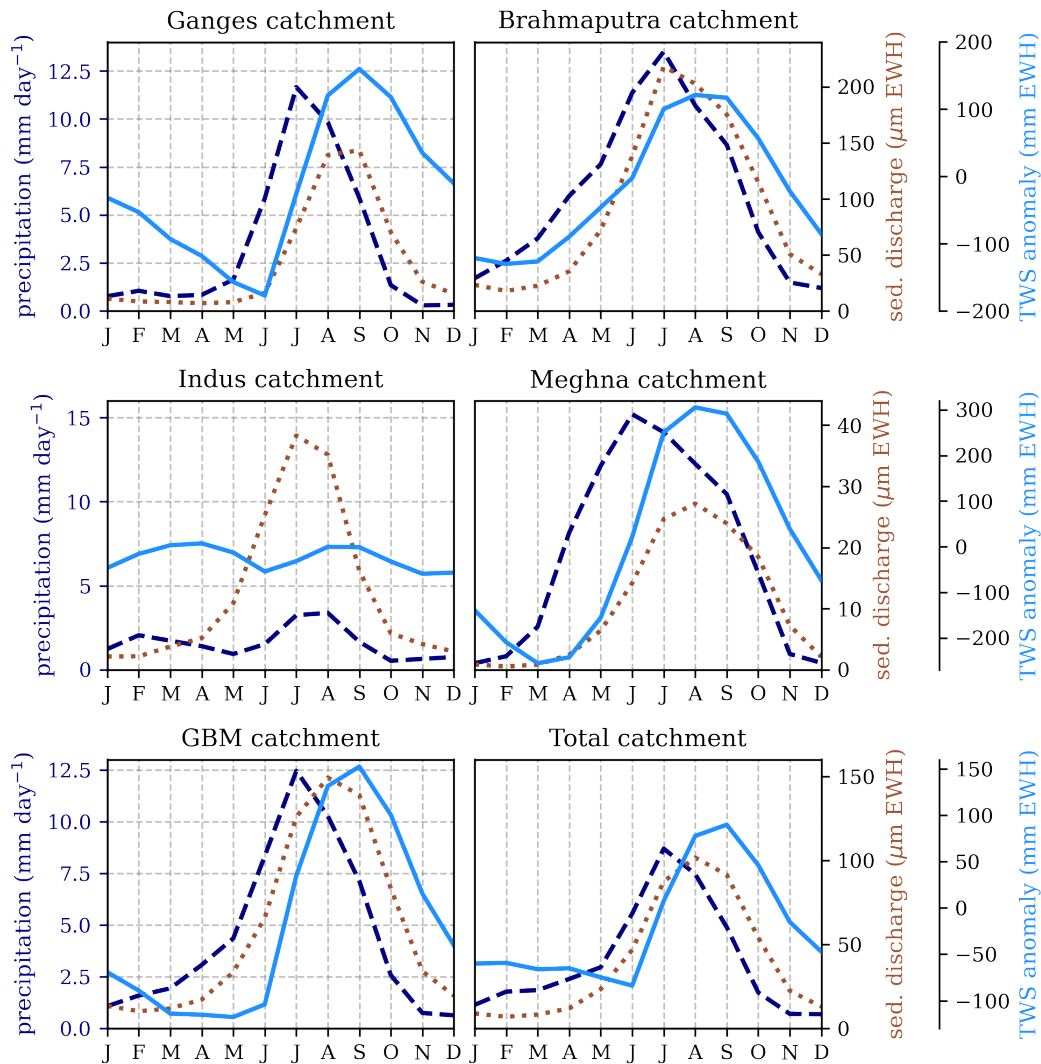


Figure 4. Average seasonality of the precipitation (dashed), the terrestrial water storage (TWS, solid), and the sediment discharge (dotted) within the individual Ganges, Brahmaputra, Indus, and Meghna catchments as well as the combined Ganges-Brahmaputra-Meghna catchment (GBM), and the total combined GBM and Indus catchments (Total). Precipitation data are averaged from the ERA5 reanalysis product for 2000-2022 (C3S, 2017). Seasonal TWS anomalies are averaged for the COST-G data product for 2002-2022 Boergens et al. (2020). Seasonality of sediment discharge is based on river water discharge according to data in Islam (2016).

February and April (Figure 4). This is likely caused by mid-latitude extra-tropical western disturbances in the southern part of the catchment (Cannon et al., 2015). The Indus sediment discharge shows only the one maximum during monsoon season.

Generally, the mass change due to sediment transport would reduce the gravimetric observations during EWH increase, while it has almost no impact on the observations during EWH decrease. In the following, however, we limit this study to an evaluation of the impact that annual sediment loss has on the gravimetric observations of reduces gravity values during TWS

increase and does not effect gravity observations during TWS decrease. However, the ~~EWH decrease~~ sediment mass loss in units of EWH show values that are by three orders of magnitude smaller than the seasonality observed in GRACE data. This monthly sediment impact is within the uncertainty of monthly gravimetry data and will not considerably impact this study's analysis. While seasonality is included in the following data, we will from here on focus on linear trends in both water and sediment loss.

3.4 Impact of sediment transport on geodetic observations of trends in ~~equivalent terrestrial water height~~ storage

Table 4. Sediment impact on gravimetric observations of TWS trends for studied catchments.

river	catchment area (km ²)	sediment loss (10 ¹² kg/yr)	GRACE TWS loss (mm/yr)	abs. sediment impact (kg/m ² /yr \approx mm/yr)	rel. sediment impact (%)
Total	2,679,069	1.28 ± 0.63	13.5 ± 2.2	0.48 ± 0.23	3.6 ± 2.3
GBM	1,576,134	1.11 ± 0.51	15.1 ± 2.7	0.70 ± 0.32	4.6 ± 3.0
Ganges	950,754	0.50 ± 0.27	16.3 ± 2.8	0.53 ± 0.29	3.3 ± 2.3
Brahmaputra	539,989	0.60 ± 0.24	14.5 ± 2.6	1.10 ± 0.44	7.6 ± 4.4
Meghna	85,391	0.011 ± 0.002	6.0 ± 4.0	0.13 ± 0.02	2.2 ± 1.8
Indus	1,102,935	0.17 ± 0.12	11.3 ± 1.9	0.15 ± 0.11	1.3 ± 1.2
Ganges-m	148,948	0.50 ± 0.27 ^(b)	15.6 ± 2.5	3.36 ± 1.83	21.5 ± 15.2
Ganges-HH	57,025	0.45 ± 0.27	15.6 ± 2.5 ^(a)	7.89 ± 4.74	50.6 ± 38.6
Ganges-LH	91,885	0.05 ± 0.05	15.6 ± 2.5 ^(a)	0.54 ± 0.54	3.5 ± 4.0
Brahmaputra-m	361,509	0.60 ± 0.24 ^(b)	16.1 ± 2.3	1.65 ± 0.66	10.3 ± 5.6
Brahmaputra-NBS	21,600	0.27 ± 0.20	16.1 ± 2.3 ^(a)	12.50 ± 9.26	77.6 ± 68.6
Brahmaputra-rem.	339,900	0.33 ± 0.22	16.1 ± 2.3 ^(a)	0.97 ± 0.65	6.0 ± 4.9

Total refers to the combined Ganges, Brahmaputra, Meghna, and Indus catchments. GBM is the Ganges-Brahmaputra-Meghna catchment. Ganges-m and Barhmaputra-m refer to the mountain regions (altitude $\geq 1,500$ m) within the Ganges and Brahmaputra catchment, respectively. Ganges-HH and Ganges-LH refer to the High Himalayas and the Lesser Himalayas in the Ganges catchment, respectively. Brahmaputra-NBS and Brahmaputra-rem. refer to the Namcha Barwa syntaxis and the remaining Brahmaputra mountains, respectively. ^(a)TWS trends within specific locations in the catchment mountain regions are approximated by the average TWS trend over the mountains. ^(b)Sediment data for the mountain regions assume all river sediment being eroded from these regions.

3.4.1 Impact within the ~~full~~ study area

To compare the mass loss from river sediment transport to the observed ~~EWH-TWS~~ trends, the absolute ~~sediment mass~~ loss is divided by the respective catchment area and the density of water. This yields the ~~absolute~~ impact of sediment mass loss in units of EWH. ~~The combined Indus, Considering the total catchment size of the Ganges, Brahmaputra, and Meghna catchments cover an area of 2,679,070 km² and experience a combined sediment mass loss of 1.3 · 10¹² kg yr⁻¹. This Meghna and Indus rivers (Table 1) as well as their combined sediment discharge (Table 3), this~~ yields an absolute sediment mass impact of roughly 0.5 mm yr⁻¹ ~~in EWH~~ that is not considered when deriving ~~the EWH of terrestrial water storage-TWS~~ based on gravimetric

observations. ~~This Accordingly, this~~ sediment mass loss needs to be subtracted from the observed ~~EWH data~~ trends in TWS anomalies, reducing the local ~~EWH trend of 1.4 cm yr^{-1}~~ TWS trend of 1.35 cm yr^{-1} by roughly 4% (Table 4, Figure 5).

~~This yields an~~The average monthly sediment impact on ~~EWH observations of~~ TWS observations is less than 0.01 cm of EWH, which is well within the uncertainties stated for ~~the GRACE EWH data within~~ GRACE TWS data in the study area (~~average EWH_{err} $\approx 1.4 \text{ cm}$~~)(~~average TWS_{std} $\approx 1.4 \text{ cm}$~~ , Boergens et al., 2020). However, considering the whole 20-year time-series, our results imply that ~~about a gravity decrease corresponding to~~ 1 cm of the observed ~~EWH decrease~~ EWH currently attributed to groundwater depletion on the Indian subcontinent could be caused by sediment transport instead(\ominus).

Exclusion of the Indus catchment yields a ~~slightly~~ stronger relative impact of sediment mass loss on the observed ~~EWH TWS~~ trend for the Ganges-Brahmaputra-Meghna catchment. This ~~can be explained~~ is caused by higher sediment discharge per catchment area ($0.70 \text{ kg m}^{-2} \text{ yr}^{-1}$ compared to $0.48 \text{ kg m}^{-2} \text{ yr}^{-1}$ Table 4). The measured ~~EWH TWS~~ decrease in the Ganges-Brahmaputra-Meghna catchment, ~~with~~ is slightly higher than for the complete study area. ~~Overall, our data yield an~~ (Figure 5). The absolute sediment impact ~~of on gravity is~~ $0.7 \text{ kg m}^{-2} \text{ yr}^{-1}$. This ~~implies that for the Ganges-Brahmaputra-Meghna catchment,~~ represents about 4.6% of the observed gravity reduction ~~in the Ganges-Brahmaputra-Meghna catchment that is~~ currently attributed to groundwater loss ~~could instead be caused by sediment transport~~ (Table 4). Over the total ~~EWH GRACE~~ data period, ~~this correction for this sediment mass loss~~ would reduce the estimated ~~EWH loss by $(1.6 \pm 0.8) \text{ cm}$~~ (supplemental Figure S7) TWS loss by about 1.6 cm.

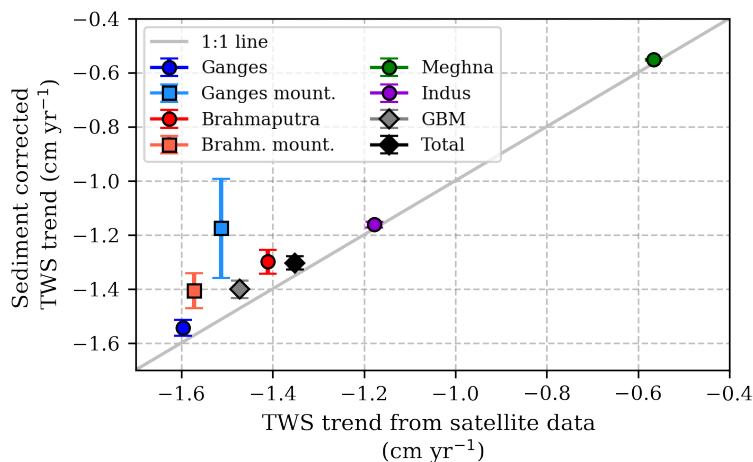


Figure 5. Time-series of EWH Comparison plot between regional trends in terrestrial water storage (TWS) derived from GRACE-COST-G data product (Boergens et al., 2020) and EWH the trends corrected for sediment mass loss. Data are averaged over points include the individual catchments as well as the combined Ganges-Brahmaputra-Meghna catchment (GBM), the total combined Indus, Ganges, Brahmputra, and Meghna catchments. Ranges for the σ -environment (Total) and the min-max estimates refer to mountain fractions of the Ganges (Ganges mount.) and Brahmputra (Brahm. mount.) catchments. Full time-series of TWS data with and without sediment estimates as stated correction are included in the supplemental figures S16 to S21.

205 3.4.2 Impact within individual catchments

Investigation of the individual river catchments yields the highest sediment mass loss for the Brahmaputra catchment (Table 4); ~~which. This~~ is consistent with the high fraction of mountains in this catchment (Table 1) and ~~the~~ high precipitation rates that enhance erosion in the Eastern Himalayas (~~Burbank et al., 2012~~)(Figure 4, ~~Burbank et al., 2012~~). The absolute sediment mass loss in the Ganges catchment is similar to that in the Brahmaputra catchment (Table 4). However, the Ganges catchment is larger
 210 than the Brahmaputra catchment, resulting in a sediment impact per catchment area that is only half that in the Brahmaputra catchment (Table 4). Sediment mass loss in the Meghna and Indus catchments is significantly lower than in the Ganges and Brahmaputra ~~catchment with only 0.13 and 0.15 kg m⁻² yr⁻¹ compared to 1.10 and 0.53 kg m⁻² yr⁻¹ catchments~~ (Table 4).

The ~~observed reduction in GRACE EWH data is highest in the Ganges catchment and lowest in the Meghna catchment (-). The fraction of the observed gravity anomalies potentially caused by Brahmaputra catchment also yields the highest relative~~
 215 ~~impact of~~ sediment mass loss ~~is highest for the Brahmaputra catchment at almost 8% on the observed gravity trend (Table 4) that would reduce the groundwater attributed EWH decline for the whole data period. Correction for this impact reduces the TWS decline by 7.8%, which over the whole GRACE data period represents more than 2 cm (-). The Indus and Meghna catchments show little impact of the sediment mass loss of 1.3% and 2.2%, respectively.~~ Figure 6). In the Ganges catchment, sediment transport ~~could be responsible for represents~~ 3.3% of these gravity anomalies that are currently attributed to groundwater
 220 ~~loss~~ the gravity decrease, and the impact within the Indus and Meghna catchments is even smaller Figure 5.

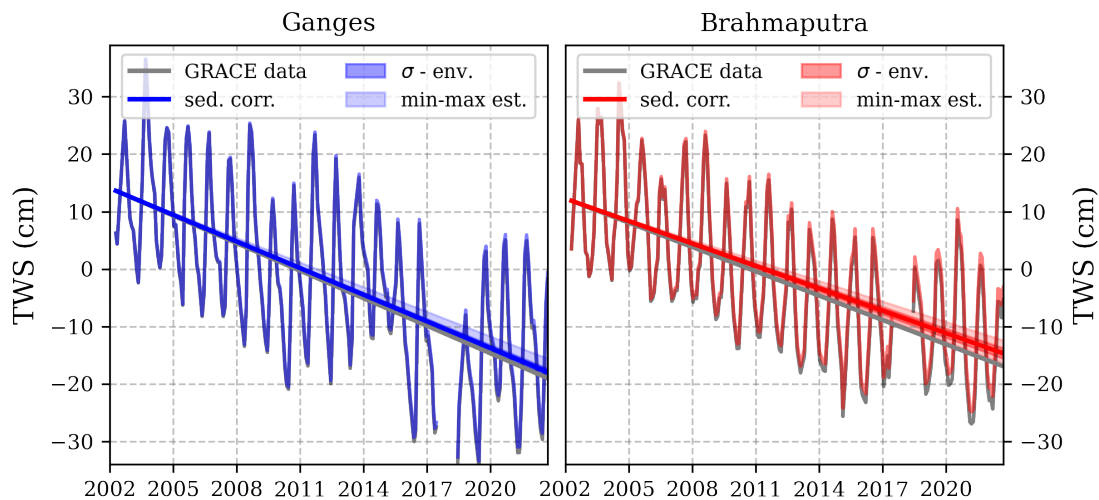


Figure 6. Time series of ~~EWH-TWS~~ derived from GRACE data (~~grey~~) and ~~EWH-TWS data~~ corrected for sediment mass loss (~~color~~). Data show average over the whole ~~Ganges (left) and Brahmaputra catchment(right) catchments~~. Ranges for the σ -environment and the min-max estimates ~~refet-refer~~ to the ~~sediment~~ standard deviation as well as minimum and maximum estimates of sediment discharge as stated in Table 3. Analogue figures for ~~the other all~~ catchments can be found in the supplemental figures ~~S8, S9 and S10~~ S16 to S21.

Sediment impact on gravimetric observations of EWH trends for studied catchments: river catchment area sediment loss
 GRACE EWH loss abs. sediment impact rel. sediment impact () () Total 2,679,070 1.28 ± 0.63 13.5 ± 2.2 0.48 ± 0.23
 3.6 ± 2.3 GBM 1,576,135 1.11 ± 0.51 15.1 ± 2.7 0.70 ± 0.32 4.6 ± 3.0 Ganges 950,754 0.50 ± 0.27 16.3 ± 2.8 0.53 ± 0.29
 3.3 ± 2.3 Brahmaputra 539,989 0.60 ± 0.24 14.5 ± 2.6 1.10 ± 0.44 7.6 ± 4.4 Meghna 85,391 0.011 ± 0.002 6.0 ± 4.0 0.13 ± 0.02
 225 2.2 ± 1.8 Indus 1,102,935 0.17 ± 0.12 11.3 ± 1.9 0.15 ± 0.11 1.3 ± 1.2 Ganges-m 148,948 $-0.50 \pm 0.27^{(b)}$ 15.6 ± 2.5 3.36 ± 1.83
 21.5 ± 15.2 Ganges-HH 57,025 0.45 ± 0.27 $15.6 \pm 2.5^{(a)}$ 7.89 ± 4.74 50.6 ± 38.6 Ganges-LH 91,885 0.05 ± 0.05 $15.6 \pm 2.5^{(a)}$
 0.54 ± 0.54 3.5 ± 4.0 Brahmaputra-m 361,509 $-0.60 \pm 0.24^{(b)}$ 16.1 ± 2.3 1.65 ± 0.66 10.3 ± 5.6 Brahmaputra-ITS 21,600
 0.27 ± 0.20 $16.1 \pm 2.3^{(a)}$ 12.50 ± 9.26 77.6 ± 68.6 Brahmaputra-rem. 339,900 0.33 ± 0.22 $16.1 \pm 2.3^{(a)}$ 0.97 ± 0.65 6.0 ± 4.9

3.4.3 Impact within the Himalayan mountain regions

230 Studies agree that the majority of sediment discharged into the Bay of Bengal is derived from the Himalaya mountain ranges (Wasson, 2003; Galy et al., 2007; Faisal and Hayakawa, 2022). Thus, we specifically studied the impact of sediment mass loss in these regions.

The Brahmaputra catchment includes a mountain fraction of 67.4% (Table 1). Assuming all of the river's sediment to be derived from these regions yields a sediment mass loss of $1.7 \text{ kg m}^{-2} \text{ yr}^{-1}$ (Table 4). ~~The average EWH~~ Considering the
 235 average TWS decrease derived from GRACE data for the region ~~is 1.6 cm yr^{-1}~~ (Table 4). ~~Thus, assuming 100% sediment origin within the Brahmaputra mountain regions,~~ the sediment mass loss accounts to roughly 10% of the ~~EWH decrease~~ currently attributed to groundwater reduction-gravity decrease (Figure 7).

According to Faisal and Hayakawa (2022), about half (45 ± 15 %) of the Brahmaputra's sediment is derived from the ~~Indus-Tsangpo suture, a tectonic suture on the northern Himalayan margin~~ Namcha Barwa syntaxis, the easternmost Himalayan
 240 syntaxis that encompasses only $\approx 4\%$ of the Brahmaputra catchment. The remaining sediment is derived from Himalayan tributaries that join the Brahmaputra in the Himalayan foreland (Faisal and Hayakawa, 2022). This indicates ~~a that~~ local sediment mass loss ~~of $12.5 \text{ kg m}^{-2} \text{ yr}^{-1}$ within the Indus-Tsangpo suture and $1.0 \text{ kg m}^{-2} \text{ yr}^{-1}$ for~~ within the Namcha Barwa syntaxis and the remaining Brahmaputra mountain areas ~~. Such mass loss represents~~ represent 78% and 6% of the observed gravity ~~anomaly in the Indus-Tsangpo suture and the remaining mountain regions~~ decrease, respectively (Table 4).

245 The Ganges catchment includes a mountain fraction of only 15.9% (Table 1). Even though sediment discharge in the Ganges river is smaller, the area weighed mass loss over the mountains ~~, with $3.4 \text{ kg m}^{-2} \text{ yr}^{-1}$,~~ is about double that of the Brahmaputra mountains (Table 4). Considering the ~~slightly higher EWH~~ higher TWS decrease in the Ganges mountains, this sediment mass loss accounts for 22% of the gravity ~~anomaly~~ decrease observed in the area (Figure 7).

According to Faisal and Hayakawa (2022), (90 ± 5)% of the Ganges sediment is derived from the High Himalayas. The
 250 remaining sediment is mostly from the Lesser Himalayas (Wasson, 2003) with a smaller contribution from intensely cultivated floodplain regions (Galy et al., 2007; Garzanti et al., 2011). Considering this, the local sediment loss from the High ~~and Lesser Himalayas~~ results to $7.9 \text{ kg m}^{-2} \text{ yr}^{-1}$ and $0.5 \text{ kg m}^{-2} \text{ yr}^{-1}$, respectively. For the High Himalayas, this Himalayas represents about half the observed gravity ~~anomaly, while for the Low~~ decrease, while in the Lesser Himalayas it is about 4% (Table 4).

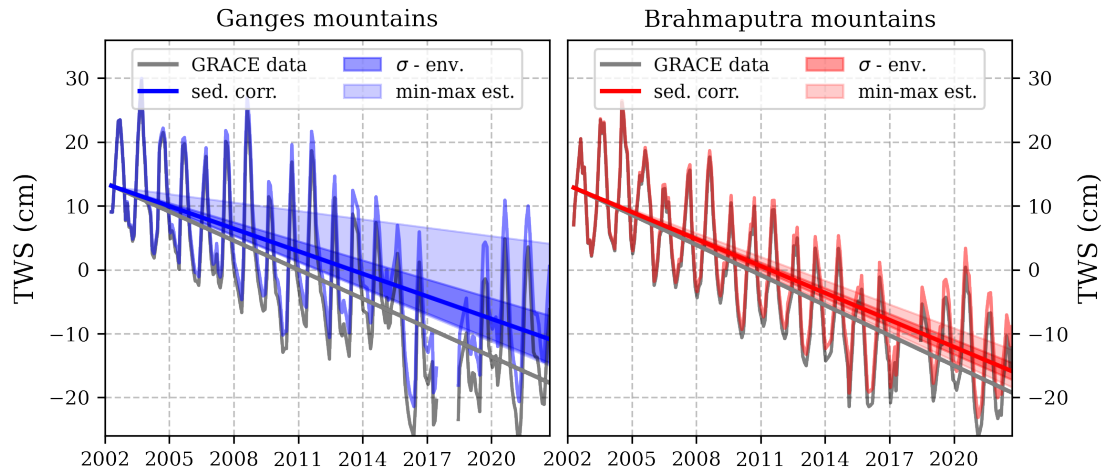


Figure 7. Time series of EWH-TWS derived from GRACE data (grey) and EWH-TWS after the correction for sediment mass loss (color). Data show average over the mountain fraction within the Ganges catchment (left) and the Brahmaputra catchment (right). σ environment and min-max estimates refer to the standard deviation as well as minimum and maximum estimates of sediment discharge as stated in Table 3. An analogous figure for the mountain sub-regions is included in the supplement as Figure SHS22.

3.4.4 Impact on agricultural within floodplain regions and observed groundwater depletion

255 Estimation To estimate the impact of sediment discharge on gravity data of groundwater depletion, we are interested in erosion within the Indo-Gangetic floodplain, where the strongest gravity decrease is observed. Generally, the estimation of the sediment impact in river lowlands and floodplains is more complicated due to sedimentary redistribution within the catchments. While some sediment might be eroded in regions of excessive agriculture (Galy et al., 2007; Garzanti et al., 2011), there might also be regions of sediment storage and river accretion. Wasson (2003) estimated the fraction of Ganges sediment discharge that was eroded from floodplain regions to be < 10%. ~~Assuming this upper estimate of~~ As an upper estimate, we assume these 10% ~~sediment being eroded from the location of the strongest observed GRACE EWH trend in southwest India of Ganges sediment to be eroded directly within the floodplain section that yields the strongest GRACE gravity reduction~~ (part of the Ganges catchment in 76°E to 79°E and 28°N to 30°N), ~~this represents~~. For this area, the sediment loss would represent a mass loss of roughly $0.9 \text{ kg m}^{-2} \text{ yr}^{-1}$ ~~that could and would~~ explain at most 2% of the observed EWH-TWS decrease in this region (5.4 cm yr^{-1}).

~~Assuming the floodplain sediment to be homogeneously eroded from the Ganges catchment located above the major aquifer in the Indo-Gangetic plain that is intensely cultivated with 88.7% agricultural region (location of aquifer is in supplemental Figure S5), the average sediment mass loss is $(0.12 \pm 0.06) \text{ kg m}^{-2} \text{ yr}^{-1}$, which represents~~ Most likely, floodplain sediment would be eroded more homogeneously from the catchment, reducing the impact to less than 1% of the observed gravity anomaly decrease. Thus, despite high sediment discharge in ~~these by~~ Indian rivers, the impact of sediment mass loss ~~impact on~~

~~EWH trends in this main region of groundwater loss seems to be insignificant.~~ on TWS trends in the floodplains is comparatively small.

3.5 Impact of the Himalaya uplift on geodetic observations of trends in terrestrial water storage

275 Sediment discharge is not the only process that impacts TWS trends from satellite gravimetry. One other process significant in the Himalayan study area is mountain orogeny. The Indian and Eurasian continental plates collide at a speed of about 50 mm yr⁻¹ (Larson et al., 1999). This causes an uplift of the Himalayan mountain range (Bisht et al., 2021) and consequentially a mass increase within this collision region. Similar to the sediment transport by rivers, such tectonic processes have so far been considered too small to be observed via satellite gravimetry (Mikhailov et al., 2004). However, like the signal of sediment transport, this gravity change becomes relevant when studying trends over long time periods.

280 While the tectonic impact on satellite gravimetry is not the focus of our study, it is relevant in order to contextualize and interpret our study as well as for potential future application of our study results. Since the Indian plate moves below the Eurasian plate, the tectonic uplift is present in the Himalayan mountain ranges and in the Tibetan Plateau but not in the Indian floodplains (Li et al., 2020). We derived an estimate of the associated mass increase based on published uplift data (Xu et al., 2000; Fu and Freymueller, 2012; Bisht et al., 2021). For the Ganges and Brahmaputra mountain ranges, we
285 find mass increases of $(0.8 \pm 1.1) \cdot 10^{12} \text{ kg yr}^{-1}$ and $(1.1 \pm 1.2) \cdot 10^{12} \text{ kg yr}^{-1}$, respectively. Details can be found in the supplemental material.

This mass increase caused by orogenic uplift in the Himalayan mountains is in the same order of magnitude as the mass reduction by the sediment transport in rivers. While both processes are present in the mountain ranges, uplift effects the full area and sediment erosion is the strongest along the river paths. However, at the current satellite resolution it is not possible
290 to separate the two processes. Thus, the gravimetric impact of tectonic processes should be studied further and needs to be combined with the impact of sediment transport before attempting a correction of TWS trends from satellite gravimetry along tectonically active mountain ranges.

4 Conclusions

Our study shows the impact of sediment erosion on gravimetric estimates of ~~terrestrial water loss within the~~ TWS loss within
295 main river catchments ~~of on~~ the Indian subcontinent. Sediment erosion within the combined Ganges, Brahmaputra, Meghna, and Indus catchments yield an average mass loss of $(0.5 \pm 0.2) \text{ kg m}^{-2} \text{ yr}^{-1}$ which potentially causes ~~roughly~~ 4% of the EWH ~~observed gravity~~ decrease currently attributed to groundwater loss. Exclusion of the Indus catchment increases the sediment impact to approximately 5%.

Comparison of ~~individual catchments yields,~~ the sediment mass loss for individual river catchments yields the highest im-
300 pact ~~of sediment mass loss is~~ for the Brahmaputra catchment ~~with~~. There, sediment mass loss is $(1.1 \pm 0.4) \text{ kg m}^{-2} \text{ yr}^{-1}$ ~~that correspond,~~ corresponding to almost 8% of the EWH ~~observed gravity~~ decrease within this catchment. In the Ganges catch-

ment, sediment transport represents 3.3% of the ~~EWH-gravity~~ decrease, while for the Meghna and Indus ~~catchment-catchments~~ its 2.2% and 1.3%, respectively.

305 ~~For mountain regions within the catchments, the regional~~ Mountain regions are especially prone to erosion. Thus, the impact
of sediment mass loss ~~is even higher on satellite gravimetry is especially important for mountain ranges~~. Over the whole Ganges
and Brahmaputra mountain ~~ranges~~range, we find sediment mass loss of $(2.2 \pm 1.0) \text{ kg m}^{-2} \text{ yr}^{-1}$ with ~~regional-average~~ loss of
 $(3.4 \pm 1.8) \text{ kg m}^{-2} \text{ yr}^{-1}$ in the Ganges mountains and $(1.7 \pm 0.7) \text{ kg m}^{-2} \text{ yr}^{-1}$ in the Brahmaputra mountains. This represents
22% and 10% of the observed ~~EWH-loss-gravity decrease~~ in the Ganges and Brahmaputra mountains, respectively. Inspection
of previously stated erosion hotspots indicates that the sediment loss could potentially explain up to 77% of the ~~EWH-gravity~~
310 ~~decrease in selected mountain regions. However, investigation of the gravity increase caused by mountain orogeny yields~~
~~data in the same order of magnitude as the gravity decrease by sediment discharge. Both processes are present mainly in the~~
~~catchment mountain fractions, and at the current satellite resolution, it is not possible to separate the two processes. Thus,~~
~~further studies of spatial distributions in sediment erosion and mountain orogeny are needed to better constrain their combined~~
~~impact on satellite gravimetry over tectonically active areas.~~

315 In the river floodplains, where gravimetric measurements show the strongest decrease, the sediment impact is ~~smaller~~~~much~~
~~smaller than over the mountains~~. The strongest ~~EWH-trend-gravity decrease~~ is observed in ~~northwest-north-west~~ India with a
reduction of up to ~~5.8 cm yr⁻¹~~~~5.8 cm of EWH per year~~. In this area, we find the sediment ~~mass-loss-impact~~ to be at most 2%
with less than 1% over the whole floodplain area.

Author contributions. AK and TW developed the concept of the study. AK performed the analysis and led the writing of the paper. MW and
320 JM contributed to the interpretation of geodetic data. TR helped interpret the sediment data. HB, JN and CL contributed to the general data
interpretation. All authors discussed results and commented on the manuscript.

Competing interests. The authors declare no competing interests.

References

- Akter, J., Roelvink, D., and van der Wegen, M.: Process-based modeling deriving a long-term sediment budget for the Ganges-Brahmaputra-Meghna Delta, Bangladesh, *Estuarine, Coastal and Shelf Science*, 260, 107–159, <https://doi.org/10.1016/j.ecss.2021.107509>, 2021.
- 325 Bisht, H., Kotlia, B. S., Kumar, K., Dumka, R. K., Taloor, A. K., and Upadhyay, R.: GPS derived crustal velocity, tectonic deformation and strain in the Indian Himalayan arc, *Quaternary International*, 575–576, 141–152, <https://doi.org/https://doi.org/10.1016/j.quaint.2020.04.028>, sI: Remote Sensing and GIS Applications in Quaternary Sciences, 2021.
- Boergens, E., Dobslaw, H., and Dill, R.: COST-G GravIS RL01 Continental Water Storage Anomalies. V. 0004., GFZ Data Services., https://doi.org/10.5880/COST-G.GRAVIS_01_L3_TWS, accessed 20.12.2022, 2020.
- 330 Borrelli, P., Robinson, D. A., Fleischer, L. R., Lugato, E., Ballabio, C., Alewell, C., Meusburger, K., Modugno, S., Schütt, B., Ferro, V., Bagarello, V., Oost, K. V., Montanarella, L., and Panagos, P.: An assessment of the global impact of 21st century land use change on soil erosion., *Nature Communications*, 8, <https://doi.org/10.1038/s41467-017-02142-7>, data accessed 10.09.2023, 2017.
- Burbank, D. W., Bookhagen, B., Gabet, E. J., and Putkonen, J.: Modern climate and erosion in the Himalaya, *Comptes Rendus Geoscience*, 344, 610–626, <https://doi.org/10.1016/j.crte.2012.10.010>, erosion–Alteration: from fundamental mechanisms to geodynamic consequences (Ebelmen’s Symposium), 2012.
- C3S: Copernicus Climate Change Service (C3S): ERA5: Fifth generation of ECMWF atmospheric reanalyses of the global climate., Copernicus Climate Change Service Climate Data Store (CDS), <https://cds.climate.copernicus.eu/cdsapp#!/home>, accessed 14.06.2022, 2017.
- Cannon, F., Carvalho, L. M. V., Jones, C., and Bookhagen, B.: Multi-annual variations in winter westerly disturbance activity affecting the Himalaya, *Climate Dynamics*, 44, 441–455, <https://doi.org/10.1007/s00382-014-2248-8>, 2015.
- 340 Cazenave, A., Dominh, K., Guinehut, S., Berthier, E., Llovel, W., Ramillien, G., Ablain, M., and Larnicol, G.: Sea level budget over 2003–2008: A reevaluation from GRACE space gravimetry, satellite altimetry and Argo, *Global and Planetary Change*, 65, 83–88, <https://doi.org/10.1016/j.gloplacha.2008.10.004>, 2009.
- Coleman, J. M.: Brahmaputra river: Channel processes and sedimentation, *Sedimentary Geology*, 3, 129–239, [https://doi.org/10.1016/0037-0738\(69\)90010-4](https://doi.org/10.1016/0037-0738(69)90010-4), brahmaputra river: Channel processes and sedimentation, 1969.
- 345 Curray, J. R.: Sediment volume and mass beneath the Bay of Bengal, *Earth and Planetary Science Letters*, 125, 371–383, [https://doi.org/10.1016/0012-821X\(94\)90227-5](https://doi.org/10.1016/0012-821X(94)90227-5), 1994.
- Dahle, C. and Murböck, M.: Post-processed GRACE/GRACE-FO Geopotential GSM Coefficients COST-G RL01 (Level-2B Product). V. 0002., GFZ Data Services., https://doi.org/https://doi.org/10.5880/COST-G.GRAVIS_01_L2B, 2020.
- 350 Dahle, C., Murböck, M., Flechtner, F., Dobslaw, H., Michalak, G., Neumayer, K. H., Abrykosov, O., Reinhold, A., König, R., Sulzbach, R., and Förste, C.: The GFZ GRACE RL06 Monthly Gravity Field Time Series: Processing Details and Quality Assessment, *Remote Sensing*, 11, <https://doi.org/10.3390/rs11182116>, 2019.
- Faisal, B. M. R. and Hayakawa, Y. S.: Geomorphological processes and their connectivity in hillslope, fluvial, and coastal areas in Bangladesh: A review, *Progress in Earth and Planetary Science*, 9, <https://doi.org/10.1186/s40645-022-00500-8>, 2022.
- 355 FAO: AQUASTAT Core Database., Food and Agriculture Organization of the United Nations., accessed via https://tableau.apps.fao.org/views/ReviewDashboard-v1/country_dashboard?%3Aembed=y&%3AisGuestRedirectFromVizportal=y (17.11.2022), 2022.
- Fu, Y. and Freymueller, J. T.: Seasonal and long-term vertical deformation in the Nepal Himalaya constrained by GPS and GRACE measurements, *Journal of Geophysical Research: Solid Earth*, 117, <https://doi.org/https://doi.org/10.1029/2011JB008925>, 2012.

- Galy, V., France-Lanord, C., Beyssac, O., Faure, P., Kudrass, H., and Palhol, F.: Efficient organic carbon burial in the Bengal fan sustained
360 by the Himalayan erosional system, *Nature*, 450, <https://doi.org/10.1038/nature06273>, 2007.
- Garzanti, E., Andó, S., France-Lanord, C., Censi, P., Vignola, P., Galy, V., and Lupker, M.: Mineralogical and chemical variability
of fluvial sediments 2. Suspended-load silt (Ganga–Brahmaputra, Bangladesh), *Earth and Planetary Science Letters*, 302, 107–120,
<https://doi.org/10.1016/j.epsl.2010.11.043>, 2011.
- Giosan, L., Constantinescu, S., Clift, P. D., Tabrez, A. R., Danish, M., and Inam, A.: Recent morphodynamics of the Indus delta shore and
365 shelf, *Continental Shelf Research*, 26, 1668–1684, <https://doi.org/10.1016/j.csr.2006.05.009>, 2006.
- GLCNMO: Global Land Cover by National Mapping Organizations: GLCNMO Version 3, Geospatial Information Authority of Japan, Chiba
University and Collaborating Organizations, accessed via https://github.com/globalmaps/gm_lc_v3 (26.10.2022), 2017.
- GRDC: Major River Basins of the World: "Major Rivers", Global Runoff Data Centre. 2nd, rev. ext. ed. Koblenz, Germany: Fed-
eral Institute of Hydrology (BfG), accessed via: [https://www.bafg.de/SharedDocs/ExterneLinks/GRDC/mrb_shp_zip.html;jsessionid=](https://www.bafg.de/SharedDocs/ExterneLinks/GRDC/mrb_shp_zip.html;jsessionid=993792470F4B2723B3942ACFA8C09C66.live11313?nn=201762)
370 [993792470F4B2723B3942ACFA8C09C66.live11313?nn=201762](https://www.bafg.de/SharedDocs/ExterneLinks/GRDC/mrb_shp_zip.html;jsessionid=993792470F4B2723B3942ACFA8C09C66.live11313?nn=201762) (24.10.2022)., 2020.
- Holeman, J. N.: The Sediment Yield of Major Rivers of the World, *Water Resources Research*, 4, 737–747,
<https://doi.org/10.1029/WR004i004p00737>, 1968.
- Islam, S.: Deltaic floodplains development and wetland ecosystems management in the Ganges–Brahmaputra–Meghna Rivers Delta in
Bangladesh, *Sustainable Water Resources Management*, 2, <https://doi.org/10.1007/s40899-016-0047-6>, 2016.
- 375 Jacob, T., Wahr, J., Pfeffer, W. T., and Swenson, S.: Recent contributions of glaciers and ice caps to sea level rise., *Nature*,
<https://doi.org/10.1038/nature10847>, 2012.
- Jarvis, A., Reuter, H., Nelson, A., and Guevara, E.: Hole-filled seamless SRTM data V4, International Centre for Tropical Agriculture (CIAT),
accessed from <https://srtm.csi.cgiar.org> (24.10.2022)., 2008.
- Jeon, T., Seo, K.-W., Youm, K., Chen, J., and Wilson, C. R.: Global sea level change signatures observed by GRACE satellite gravimetry,
380 *Scientific Reports*, 8, <https://doi.org/10.1038/s41598-018-31972-8>, 2018.
- Kuehl, S. A., Allison, M. A., Goodbred, S. L., and Kudrass, H.: The Ganges-Brahmaputra Delta, in: *River Deltas–Concepts, Models, and
Examples*, SEPM Society for Sedimentary Geology, <https://doi.org/10.2110/pec.05.83.0413>, 2005.
- Larson, K. M., Bürgmann, R., Bilham, R., and Freymueller, J. T.: Kinematics of the India-Eurasia collision zone from GPS measurements,
Journal of Geophysical Research: Solid Earth, 104, 1077–1093, <https://doi.org/https://doi.org/10.1029/1998JB900043>, 1999.
- 385 Lehner, B. and Grill, G.: Global river hydrography and network routing: baseline data and new approaches to study the world’s large river
systems., <https://doi.org/10.1002/hyp.9740>, accessed via <https://www.hydrosheds.org/products/hydrobasins> (20.10.2022), 2013.
- Li, L., Murphy, M. A., and Gao, R.: Subduction of the Indian Plate and the Nature of the Crust Beneath Western Tibet: Insights From Seis-
mic Imaging, *Journal of Geophysical Research: Solid Earth*, 125, e2020JB019 684, <https://doi.org/https://doi.org/10.1029/2020JB019684>,
e2020JB019684 2020JB019684, 2020.
- 390 Li, Z., Zhang, Z., Scanlon, B. R., Sun, A. Y., Pan, Y., Qiao, S., Wang, H., and Jia, Q.: Combining GRACE and satel-
lite altimetry data to detect change in sediment load to the Bohai Sea, *Science of The Total Environment*, 818, 151677,
<https://doi.org/10.1016/j.scitotenv.2021.151677>, 2022.
- Luthcke, S. B., Sabaka, T., Loomis, B., Arendt, A., McCarthy, J., and Camp, J.: Antarctica, Greenland and Gulf of Alaska land-ice evolution
from an iterated GRACE global mascon solution, *Journal of Glaciology*, 59, 613–631, <https://doi.org/10.3189/2013JoG12J147>, 2013.

- 395 Mahmud, M. I., Mia, A. J., Islam, M. A., Peas, M. H., Farazi, A. H., and Akhter, S. H.: Assessing bank dynamics of the Lower Meghna River in Bangladesh: an integrated GIS-DSAS approach, *Arabian Journal of Geosciences*, 13, <https://doi.org/10.1007/s12517-020-05514-4>, 2020.
- Mikhailov, V., Tikhotsky, S., Diament, M., Panet, I., and Ballu, V.: Can tectonic processes be recovered from new gravity satellite data?, *Earth and Planetary Science Letters*, 228, 281–297, <https://doi.org/https://doi.org/10.1016/j.epsl.2004.09.035>, 2004.
- 400 Milliman, J. D. and Meade, R. H.: World-Wide Delivery of River Sediment to the Oceans, *The Journal of Geology*, 91, 1–21, <http://www.jstor.org/stable/30060512>, 1983.
- Mouyen, M., Longuevergne, L., Steer, P., Crave, A., Lemoine, J.-M., Save, H., and Robin, C.: Assessing modern river sediment discharge to the ocean using satellite gravimetry, *Nature Communications*, 9, <https://doi.org/10.1038/s41467-018-05921-y>, 2018.
- Panda, D. K. and Wahr, J.: Spatiotemporal evolution of water storage changes in India from the updated GRACE-derived gravity records, 405 *Water Resources Research*, 52, 135–149, <https://doi.org/10.1002/2015WR017797>, 2016.
- Rahman, M., Dustegir, M., Karim, R., Haque, A., Nicholls, R. J., Darby, S. E., Nakagawa, H., Hossain, M., Dunn, F. E., and Akter, M.: Recent sediment flux to the Ganges-Brahmaputra-Meghna delta system, *Science of The Total Environment*, 643, 1054–1064, <https://doi.org/10.1016/j.scitotenv.2018.06.147>, 2018.
- Rodell, M., Velicogna, I., and Famiglietti, J. S.: Satellite-based estimates of groundwater depletion in India, *Nature*, 460, 410 <https://doi.org/10.1038/nature08238>, 2009.
- Rodell, M., Famiglietti, J. S., Wiese, D. N., Reager, J. T., Beaudoin, H. K., Landerer, F. W., and Lo, M.-H.: Emerging trends in global freshwater availability, *Nature*, 557, <https://doi.org/10.1038/s41586-018-0123-1>, 2018.
- Schnitzer, S., Seitz, F., Eicker, A., Güntner, A., Wattenbach, M., and Menzel, A.: Estimation of soil loss by water erosion in the Chinese Loess Plateau using Universal Soil Loss Equation and GRACE, *Geophysical Journal International*, 193, 1283–1290, 415 <https://doi.org/10.1093/gji/ggt023>, 2013.
- Siebert, S., Burke, J., Faures, J. M., Frenken, K., Hoogeveen, J., Döll, P., and Portmann, F. T.: Groundwater use for irrigation – a global inventory, *Hydrology and Earth System Sciences*, 14, 1863–1880, <https://doi.org/10.5194/hess-14-1863-2010>, 2010.
- Smith, G. S., Best, J. L., Bristow, C. S., and Petts, G. E.: Braided Rivers: process, deposits, ecology and management., <https://www.wiley.com/en-us/Braided+Rivers:+Process,+Deposits,+Ecology+and+Management-p-9781444304374>, 2009.
- 420 Subramanian, V. and Ramanathan, A. L.: Nature of Sediment Load in the Ganges-Brahmaputra River Systems in India, pp. 151–168, Springer Netherlands, Dordrecht, https://doi.org/10.1007/978-94-015-8719-8_8, 1996.
- Tiwari, V. M., Wahr, J., and Swenson, S.: Dwindling groundwater resources in northern India, from satellite gravity observations, *Geophysical Research Letters*, 36, <https://doi.org/https://doi.org/10.1029/2009GL039401>, 2009.
- Wada, Y., van Beek, L. P. H., and Bierkens, M. F. P.: Nonsustainable groundwater sustaining irrigation: A global assessment, *Water Resources 425 Research*, 48, <https://doi.org/10.1029/2011WR010562>, 2012.
- Wasson, R. J.: A sediment budget for the Ganga–Brahmaputra catchment, *Current Science*, 84, 1041–1047, <http://www.jstor.org/stable/24107666>, 2003.
- Wilson, C. A. and Goodbred, S. L.: Construction and Maintenance of the Ganges-Brahmaputra-Meghna Delta: Linking Process, Morphology, and Stratigraphy, *Annual Review of Marine Science*, 7, 67–88, <https://doi.org/10.1146/annurev-marine-010213-135032>, PMID: 25251271, 430 2015.

Xie, H., Longuevergne, L., Ringler, C., and Scanlon, B.: Integrating groundwater irrigation into hydrological simulation of India: Case of improving model representation of anthropogenic water use impact using GRACE, *Journal of Hydrology: Regional Studies*, 29, 100681, <https://doi.org/10.1016/j.ejrh.2020.100681>, 2020.

435 Xu, C., Liu, J., Song, C., Jiang, W., and Shi, C.: GPS measurements of present-day uplift in the Southern Tibet, *Earth, Planets and Space*, 52, 735–739, <https://doi.org/10.1186/BF03352274>, 2000.